Available online at www.sciencedirect.com

ScienceDirect

Procedia - Social and Behavioral Sciences 104 (2013) 1130 – 1138

Procedia
Social and Behavioral Sciences

2nd Conference of Transportation Research Group of India (2nd CTRG)

Comparative analysis of pedestrian, bicycle and car traffic moving in circuits

Jun Zhang[a]*, Wolfgang Mehner[a], Erik Andresen[b], Stefan Holl[a,b], Maik Boltes[a], Andreas Schadschneider[c], Armin Seyfried[a,b]

[a]*Jülich Supercomputing Centre, Forschungszentrum Jülich GmbH 52425 Jülich, Germany*
[b]*University of Wuppertal, Pauluskirchstraße 7. 42285 Wuppertal, Germany*
[c]*Institut für Theoretische Physik, Universität zu Köln. 50937 Köln, Germany*

Abstract

In this study, we provide results of controlled experiments of single file bicycle movement on a circuit. We compare the fundamental characteristics of bicycle traffic with that of car and pedestrian traffic, which have been studied extensively in previous research under similar condition. From the comparison of the time-space diagrams of these three one-dimensional traffic flows, different states of motion (free flow state, the jammed state and stop-and-go waves) can be observed in all these systems. The fundamental diagrams are compared in two different ways. Without considering the size and free velocity of these three kinds of objects, the data points occupy different density ranges in the diagram. However, when we use the concept of scaling by considering the free velocity and size of the moving objects, the fundamental diagrams show the same structure and values. This implies that the transport properties in these three different types of single file traffic flow could be unified in a certain range by simple scaling. These results provide insights into the dynamics but also may be relevant for the improvement of mixed traffic systems.

Selection and peer-review under responsibility of International Scientific Committee.

Keywords: bicycle traffic; fundamental diagram; mixed traffic; pedestrian experiment.

1. Introduction

Recently, green and convenient transportation is being promoted due to traffic and environment problems. Thus, usage of bicycle is encouraged in most countries. In this situation, mixed traffic with pedestrians, bicycles

* Corresponding author. Tel.: +49 2461 61 1995; fax: +49 2461 61 6656.
E-mail address: ju.zhang@fz-juelich.de

1877-0428 © 2013 The Authors. Published by Elsevier Ltd.
Selection and peer-review under responsibility of International Scientific Committee.
doi:10.1016/j.sbspro.2013.11.209

as well as motorized vehicles would be much more complex and difficult to plan, which sets higher demands upon an optimized design of urban traffic systems. To improve the traffic flow and road capacity for this kind of mixed traffic, it is necessary to understand the characteristics of these three different kinds of traffic as well as the relationship between them.

In the past, a lot of studies have been done on pedestrian (Helbing and others, 2005; Schadschneider and others, 2009), bicycle (Taylor & Davis, 1999) and vehicle traffic (Chowdhury and others, 2000; Nagatani, 2002; Kerner, 2004). Usually these traffic flows are investigated separately. Most of the methods and theories in pedestrian dynamics are borrowed from vehicular traffic. As for the study of bicycle traffic, most research focuses on operating characteristics, travel speed distributions as well as bicycle characteristics. Limited studies were carried out to derive the fundamental diagram of bicycle flow (Smith, 1976; Navin, 1994; Andresen and others, 2013). On the other hand, modern traffic is usually characterized by a mixture of vehicles, pedestrians, and bicycles. Some studies on the interactions between different transportation modes also appear. Katz et al. (1975) conducted controlled experiments to study driver and pedestrian interaction during the crossing conflict. Different variables were combined in a complete factorial design. They tried to find the condition when drivers would slow down or stop for crossing pedestrians. Jiang et al. (2006) studied the interaction between vehicles and pedestrians in narrow channel numerically. Cheng et al. (2008) and Yao et al. (2009) proposed models to simulate conflicts in vehicle-bicycle traffic flow. Ma et al. (2011) adopted an extended finite-grid cellular automaton model to study the dynamic features of pedestrian-vehicle conflicts. It is found that the presence of vehicles has made the mixed traffic system unstable and increases the probability of transiting from free flow to perfect stop. However, the similarities and differences among the fundamental diagrams of these three traffic modes are rarely investigated. Nearly all studies on pedestrians and vehicles show that traffic flow at a certain critical value of density is unstable and transits from free flow to jammed flow. However, the similarities of the three kinds of driven systems are rarely investigated. It is still not known whether the empirical experience from pedestrian and car flow can be used in bicycle flow, or whether the fundamental diagrams of these three kinds of flow can be unified into one diagram in certain situations.

Collecting empirical data with a consistent and systematic methodology is a priority for research, facility design and policy making. The capacities of traffic routes are necessary for safety and risk assessment as well as model calibration. In this work, single file pedestrian, bicycle and car movement in a circuit on plane ground will be studied under laboratory conditions. To regulate global density inside the circular road, series of runs were carried out and the number of agents were changed each run. The maximal numbers of participants in these experiments are 34, 33 and 23 for pedestrian, bicycle and car experiment respectively. All of them were asked to move at normal speed without overtaking. Under similar conditions, we will compare the fundamental diagrams of these three kinds of traffic flow. We try to find a condition to unify them in one diagram and understand the corresponding mechanism.

The remainder of the paper is organized as follows. In Section 2 we describe the setup of the experiments. Section 3 analyzes the characteristics of these traffic flows based on trajectories extracted from video recordings and shows the main results. Finally, the conclusions from our investigation will be discussed.

2. Experiment setup

All three experiments were carried out in circuits on plane ground. Several runs were performed by changing the number of participants who were asked to move normally without overtaking. In the following sections, details of these experiments will be described.

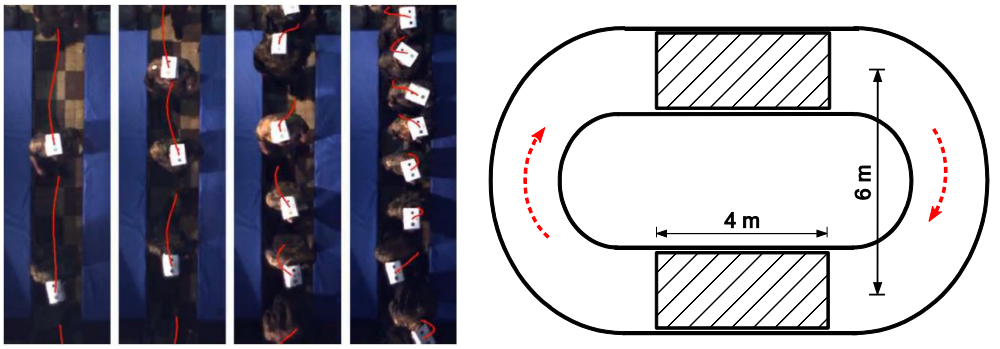

Fig. 1. Snapshot and sketch of the pedestrian experiment in Germany.

2.1. Pedestrian experiment

Fig. 1 shows snapshots and a sketch of the pedestrian experiment. This experiment was performed in 2006 in the wardroom of Bergische Kaserne Düsseldorf in Germany. The circumference of the corridor was about C = 26 *m* in length and the participants were female and male soldiers. Pasteboards with high contrast markers were put on the head of each soldier for trajectory extraction. To get different ranges of global density in the corridor, 12 runs with the number of test persons N = 14, 17, 20, 22, 25, 28, 34, 39, 45, 56, 62, 70 were performed. This means that the global density (ρ_g = N/C) ranges from 0.54 to 2.69 m^{-1} in this experiment. Two cameras were used to record the pedestrian movement in the two 4 *m* length areas with a frame rate of 25 *fps*. Detailed information about this experiment can be found in Seyfried et al. (2010).

2.2. Bicycle experiment

Fig. 2(a) is a snapshot of the bicycle experiment, which was carried out in Germany in 2012. All of the participants in this experiment, composed of children and adults, were volunteers recruited by advertisement. The youngest and oldest participants were 11 and 66 years old. The mean height of them was 1.75 ± 0.14 *m*. The mean length of the bicycles was 1.73 ± 0.12 *m*. The mean weight of each participant plus his/her bicycle was 85.4 ± 25.3 *kg*. To make trajectory extraction easier afterwards, all participants were asked to wear a helmet with yellow safety hat coverings. The circuit road was drawn on the plane ground with a circumference of 86 *m*. The participants were asked to ride inside the circuit without overtaking during the experiment. Eight runs were performed with a different number of bicycles N = 5, 7, 10, 15, 18, 20, 33, 33 in each run. In the first seven runs the participants were asked to ride in anticlockwise direction, whereas a run was carried out clockwise with all the 33 participants at the end. The frame rate of the camera is also 25 *fps* in this experiment.

Fig. 2. Snapshots of (a) the bicycle experiment in Germany and (b) the car experiment in Japan (Nakayama and others, 2009).

2.3. Car experiment

Fig. 2(b) displays a snapshot of the car experiment on a circuit road with circumference 230 *m*. It is worth noting that it was carried out by Sugiyama et al. in Japan and the circuit is a circle. Before the experiment, drivers were asked to cruise at about 30 *km/h* with almost uniform spacing. After the start of a run, they were only asked to follow the vehicle ahead in safety without any other instruction. A total of two runs were carried out with the number of cars N = 22 and 23 inside the circuit, which means the global densities ρ_g were 0.096 and 0.1 m^{-1} respectively. The whole path of each car was recorded with a frame rate of 3 *fps* in this experiment. Details about this experiment can be found in Sugiyama et al. (2008) and Nakayama et al. (2009).

3. Results and analysis

3.1. Trajectory extraction

The trajectory extraction methods for the pedestrian and car experiments have already described in Boltes et al. (2010) and Sugiyama et al. (2008) in detail. In this section, we only explain the extraction method for the bicycle experiment. The bicycle experiment was filmed using two cameras and the trajectories were extracted automatically. In order to facilitate automatic tracking, the participants wore yellow helmets. Additionally their bicycles were fitted with special markers, which were attached to the luggage carriers. Each marker is different from the others and can be used to identify each participant. The first camera captures a top view, overseeing the whole setup. In order to read out the markers, a second camera was used and was positioned much closer to the participants. It only provides a partial view of the oval.

The helmets and markers are detected using standard methods from computer vision, such as Chamfer matching and Differences of Gaussians (to detect bright circular shapes in front of a dark background). After detection, the objects are tracked using Kalman filters (Forsyth and Ponce, 2003) and their 3D coordinates are computed. In case of the top view, a virtual plane 1.75 meters above the ground level is used. Rays are cast and intersected with this plane for each detection. The height of 1.75 meters is the average size (distance from ground to helmet) of the participants. Once the markers are read out and the identity of each participant becomes known,

an individual plane for each participant can be used, where the height above ground corresponds to the participants' size.

3.2. Time-Space diagram

From the high precision trajectories, traffic flow characteristics including flow, density and velocity can be determined. Fig. 3 to 5 show time-space diagrams from some runs of these experiments. In these graphs, instantaneous velocities $v_i(t)$ of each object are also exhibited. For the pedestrian and bicycle experiment, we can only show the trajectories inside the recording areas which are 4 *m* and 27 *m* respectively. For the car experiment, however, the trajectories over the entire 230m circuit road are shown.

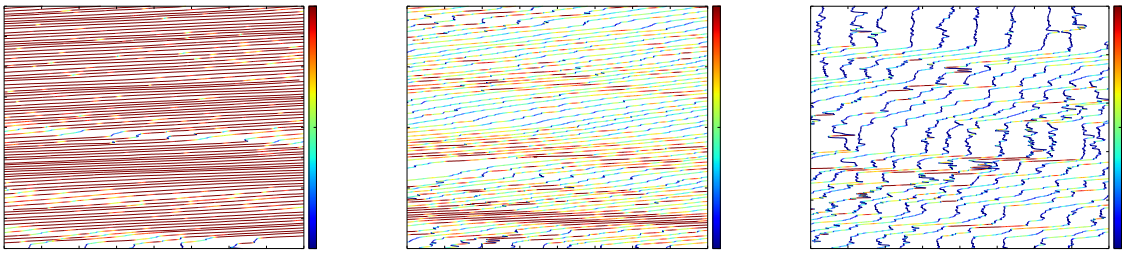

a) N_{ped} = 39 b) N_{ped} = 56 c) N_{ped} = 70

Fig. 3. Time-space diagram of the pedestrian experiment.

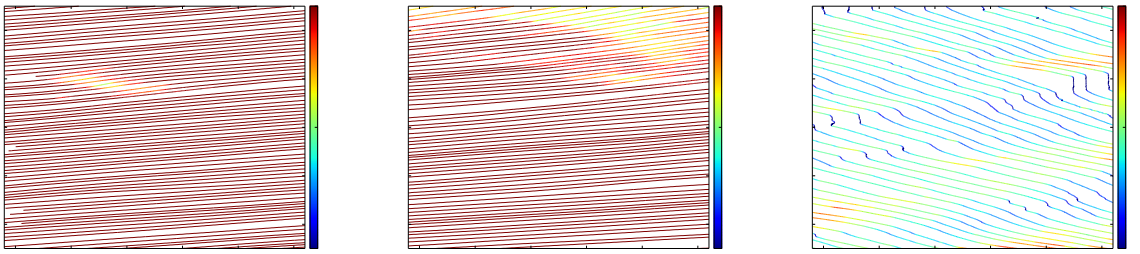

a) $N_{bicycle}$ = 20, Anticlockwise b) $N_{bicycle}$ = 33, Anticlockwise c) $N_{bicycle}$ = 33, Clockwise

Fig. 4. Time-space diagram of the bicycle experiment.

In Fig. 3, runs with the number of pedestrians N = 39, 56 and 70, which represents the global densities 1.50, 2.15 and 2.69 m^{-1}, are depicted. The transformation from free movement state to jamming state can be observed. Especially when the global density is 2.69 m^{-1}, stop-and-go wave is so obvious that pedestrian can hardly move and stop states domain nearly the entire run.

Fig. 4 shows three runs of the bicycle experiment with 20 and 33 participants (corresponding to global densities 0.23 and 0.38 m^{-1}), respectively. In the case of anti-clockwise movement no congestion can be observed up to N = 33, although there are fluctuations of local velocities which become much more apparent with the increase of the number of participants inside the circuit. However, Fig. 4 (b) and (c) show considerable differences, even though the number of participants inside the scenario is the same. The stop-and-go wave is observed when the 33 participants were asked to ride in clockwise direction. On one hand, this may be caused by

the different flexibility of right and left hands. On the other hand, the participants have ridden in anti-clockwise for a few runs and they have adapted well with this direction. When they were asked to ride in opposite direction then, they have to regulate their driving behavior again. This may be another reason for this difference. However, from current data we are not able to identify the cause of this surprising discrepancy which still needs further investigation.

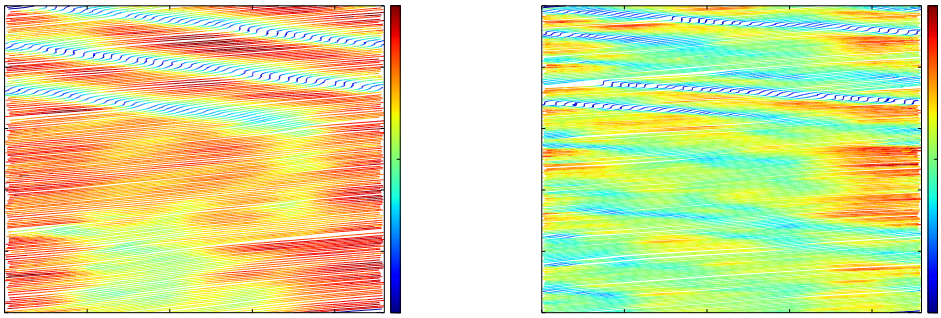

a) $N_{car} = 22$ b) $N_{car} = 23$

Fig. 5. Time-space diagram of the car experiment.

Finally we consider the same type of experiment with cars. Fig. 5 shows the time-space diagrams of the two runs with 22 and 23 cars inside the circle circuit. Jams as well as their backward propagation can be observed in both of these two runs. Compared to the run with N = 23, however, the average local velocity is higher and the movement is much more stable for N = 22. The jam formation seems to be triggered by some disturbance which is time and density dependent. At high density situations, such disturbances occur much easier and more frequently. As discussed in Nakayama et al. (2009), once a jam appears it will occur again and again even if a driver dissolves the jam once.

3.3. Fundamental diagram

By comparing the time-space diagrams, we have found some qualitative similarities among these three systems. To gain a deeper understanding, quantitative analysis is indispensable to uncover the underlying dynamics that is not apparent through simple observation. The fundamental diagram, as the basic relationship in traffic engineering, should be considered first. However, the measured variables from different methods vary a lot, e.g. depending on the type of averaging used. According to our previous studies on two dimensional pedestrian experiments, the Voronoi-based method has the advantage of high spatial resolution and smaller fluctuations of measured densities compared to other methods (Steffen and others, 2010; Zhang and others, 2011). At a macro level, we therefore use the concept of Voronoi method in this study.

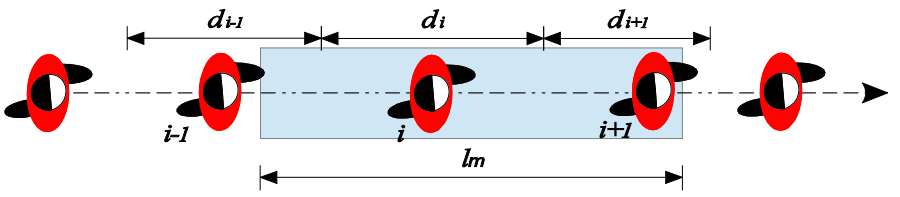

Fig. 6. Inllustration of the Voronoi method in one dimensional space. The gray region shows the measurement area.

In two-dimensional spaces, the Voronoi space of a pedestrian is obtained based on the coordinates of the neighbors around him. Similarly, in the one-dimensional case we calculate the Voronoi space d_i of pedestrian i based on the coordinates of his two neighbors i-1 and i+1. Actually, the length of d_i is half the distance between the two neighbors (see Fig. 6). In this method, a measurement area with the length of l_m is selected to calculate the Voronoi density $\langle\rho\rangle_v(t)$ and velocity $\langle v\rangle_v(t)$.

$$\langle\rho\rangle_v(t)=\frac{\sum_{i=1}^{n}\Theta_i(t)}{l_m} \quad \text{and} \quad \langle v\rangle_v(t)=\frac{\sum_{i=1}^{n}\Theta_i(t)\cdot v_i(t)}{l_m}$$

Here n is the number of pedestrians whose Voronoi space overlaps the measurement area (assuming the overlapping length is d_{oi} for pedestrian i). $\Theta_i(t)= d_{oi}/ d_i$ represents the contribution of pedestrian i to the density of the measurement area. $v_i(t)$ is the instantaneous velocity of pedestrian i at time t. It is calculated by using the displacement in a small time interval $\Delta t'$ around t, that is

$$v_i(t)=\frac{x_i(t+\Delta t'/2)-x_i(t-\Delta t'/2)}{\Delta t'}$$

For the comparison, the measurement areas for these three experiments are selected as follows: from x = -1.5 m to x = 1.5 m for the pedestrian experiment, from x = 25 m to x = 38 m for the bicycle experiment and from x = 100 m to x = 135 m for the car experiment. With such a selection, at most 7 pedestrians, bicycles or cars can exist in the area at the same time according to the length of medium cars 4.7 m, bicycle 1.73 m and pedestrian 0.43 m. It could be interesting that the ratios between the agent length and the length of the system are in the same order of magnitude in these experiments. The time interval $\Delta t'$ = 2 s is selected to calculate the velocity.

As shown in the time-space diagrams, three different states (free flow state, congestion without and with stop-and-go wave) can be observed in all of these systems. But the data in each state is still insufficient to get a complete fundamental diagram. Most data in the car experiment belongs to the congestion state without stop-and-go waves. From the bicycle experiment only few data points are obtained in the congestion state with stop-and-go waves. For the pedestrian experiment we have a wide range of data which covers all three states.

In Fig. 7 (a) we plot the fundamental diagrams of these three systems directly in one graph. The data points occupy different ranges of density and do not seem to be comparable to each other. However, when we use the concept of scaling by considering the free velocity and size of the moving objects, the fundamental diagrams look much more similar (see Fig. 7(b) and (c)). As for the length of each object, we take d_0 = 0.43 m for pedestrians, the mean value d_0 = 1.73 m for bicycles and d_0 = 4.7 m for cars which is the length of an average car. The second aspect that we consider is the free speed of each agent. From the microscopic analysis, we know that they are about 1.4 m/s for pedestrians and 5.5 m/s for bicycles in the experiment. However, there is no data on the free velocity of cars in the circuit. Here we use 14.5 m/s (about 52.2 km/h) which seems to be reasonable. After

considering these two factors, it is found that the scaled fundamental diagram, especially for bicycles and pedestrians, agree well in the density ranges observed. Furthermore, the critical densities (approximately ρd_0 = 0.45 and 0.71) where the flow transfers from one state to the next state also fit well. This implies that the transition of the flow to the congested state occurs when 45% of the available space is occupied. Stop-and-go wave will occur at an occupation of 71%.

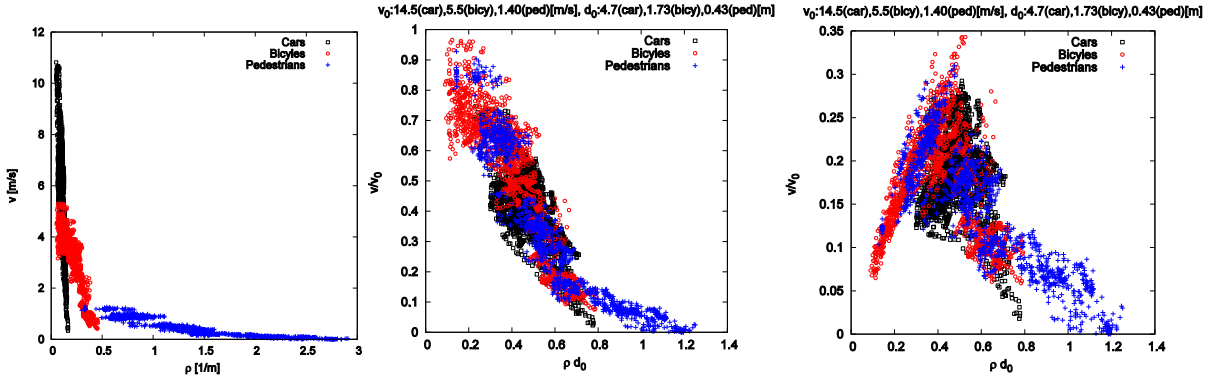

Fig. 7. Comparison of the fundamental diagrams of car, bicycle and pedestrian movement in a circuit. (a) density-velocity relationship without considering the scaling concept; (b) scaled density-velocity relationship; (c) scaled density-flow relationship.

In Fig. 7(c), the specific flow in the stop-and-go state can be maintained in the range from 0.7 to 0.9 and then decreases to zero for pedestrian traffic. An important point that should be noticed is the range of scaled densities $\rho \cdot d_0$, the maximum of which is beyond 1.0 for pedestrians. In these experiments no notable body contact was observable and the compressibility of human bodies is not responsible for this effect. Instead pedestrian trajectories in this study are extracted by detecting the markers on the head pasteboards but not the real center of mass of pedestrian. Head movement in combination with evasion to side to avoid contacts and the restriction of the trajectories in one dimension for this comparative analysis is responsible for values of the rescaled density higher than 1. For bicycles, there could be some overlapping at higher density situation, which may cause the value of scale density beyond or closer to 1.0. However, this may be impossible for car traffic, since cars have to keep certain distance to avoid potential collisions. This implies that some differences could be observed at congestion state with stop-and-go waves. How large can the scaled density achieve is still not know from the current experiment.

From the above discussion, we can conclude that the transport properties of these three different types of single file traffic flows can be unified in a certain range by simple scaling of densities and velocities. The potential difference can appear at the stop-and-go state and should be verified by further experiments.

Summary

Series of experiments with single file bicycle traffic were carried out on a circuit road on plane ground. We compare the fundamental characteristics of one-dimensional movement of bicycles with that of pedestrian and car traffic under similar conditions. All runs of experiments were recorded by video cameras and the trajectories of the moving objects were extracted from videos. Based on these trajectories, we analyze the relationship between density, velocity and flow using the same measurement method for all experiments. In all the three kinds of traffic systems, jammed states and stop-and-go waves are observed. However, in our bicycle experiment these waves only occur when the participants ride in clockwise direction at high density. The fundamental diagrams are compared in two different ways. Without considering the size and free velocity of these three kinds of objects,

the data points occupy different regions in the diagram. The density ranges are about 0.3 ~ 2.8 m^{-1}, 0.07 ~ 0.45 m^{-1} and 0.05 ~ 0.2 m^{-1} for pedestrians, bicycles and cars respectively. While the velocity ranges are 0.05 ~ 1.3 *m/s*, 0.7 ~ 5.7 *m/s* and 2.2 ~ 10.5 *m/s*. However, when we use the concept of scaling by considering the free velocity and size of the moving objects, the fundamental diagrams become much more similar.

Summarizing, we have shown that the transport properties of these three different types of single file traffic flows can be unified in a certain range by simple scaling of velocity and density. These results may not only provide insights into dynamical behavior but also may be relevant for the improvement of mixed traffic systems. However, to investigate this point further empirical data is still needed especially in the higher density range for bicycle traffic and lower density range for cars.

References

Andresen, E., Seyfried, A. & Huber, F. (2013). Basic driving dynamics of cyclists. 1st SUMO user conference 2013. pp.195-204.

Boltes, M., Seyfried, A. Steffen, B. & Schadschneider, A. (2010). Automatic extraction of pedestrian trajectories from video recordings. *Pedestrian and Evacuation Dynamics 2008*, Proceedings of the International Conference. Springer (Berlin), pp. 43-54.

Cheng, S.H., Yao, D.Y., Zhang, Y., Su, Y.L., Xu, W.D. (2008). A CA model for intrusion conflicts simulation in vehicles-bicycles laminar traffic flow. In: *Proceedings of the 11th International IEEE Conference on Intelligent Transportation Systems Beijing*, China.

Chowdhury, D., Santen, L. & Schadschneider, A. (2000). Statistical physics of vehicular traffic and some related systems. *Physics Reports*, 329, pp. 199-329.

Forsyth, D. A. & Ponce., J. (2003). Computer vision: a modern approach. *Prentice Hall*.

Helbing, D., Buzna, L., Johansson, A. & Werner, T. (2005) Self-organized pedestrian crowd dynamics: experiments, simulations, and design solutions. *Transportation Science*. 39, 1-24.

Jiang, R. & Wu, Q.S. (2006). Interaction between vehicle and pedestrians in a narrow channel. *Physica A*, 368, 239 -246.

Katz, A., Zaidel, D. & Elgrishi, A. (1975). An experimental study of driver and pedestrian interaction during the crossing conflict. *Human Factors*. 17(5), 514-527

Kerner, S. (2004). Empirical freeway pattern features, *Engineering Applications, and Theory*.

Ma, J., Lo, S., Xu, X. & Song, W. (2011) Dynamic features of pedestrian-vehicle counter flow conflicts. *ICTE 2011*: pp. 697-702.

Nagatani, T. (2002). The physics of traffic jams. *Reports on Progress in Physics*, 65, pp. 1331-1386.

Nakayama, A., Fukui, M., Kikuchi, M., Hasebe, K., Nishinari, K., Sugiyama, Y. et al.. (2009). Metastability in the formation of an experimental traffic jam. *New Journal of Physics*, 11, p.083025.

Navin, F., (1994). Bicycle Traffic Flow Characteristics: Experimental Results and Comparisons. *ITE Journal*, pp. 31–36.

Schadschneider, A., Klingsch, W., Klüpfel, H., Kretz, T., Rogsch C. & Seyfried, A. (2009). Evacuation dynamics: empirical results, modeling and application. In Robert A. Meyers (Ed), *Enzyclopedia of Complexity and System Science*, ISBN: 978-0-387-75888-6, vol. 3, pp. 3142, Springer.

Seyfried, A., Portz, A., & Schadschneider, A. (2010). Phase coexistence in congested states of pedestrian dynamics. In *Cellular Automata, ser. Lecture Notes in Computer Science*, S. Bandini, S. Manzoni, H. Umeo, and G. Vizzari, Eds., vol. 6350, *9th International Conference on Cellular Automata for Reseach and Industry*, ACRI 2010 Ascoli Piceno, Italy. Springer Berlin Heidelberg, pp. 496–505.

Smith, D., (1976). Safety and locational criteria for bicycle facilities. *Report FHWA-RD-75-112*. FHWA, U.S. Department of Transportation.

Steffen, B. & Seyfried, A. (2010). Methods for measuring pedestrian density, flow, speed and direction with minimal scatter, *Physica A*. 389, 1902-1910

Sugiyama, Y., Fukui, M., Kikuchi, M., Hasebe, K., Nakayama, A., Nishinari, K. et al.. (2008) Traffic jams without bottlenecks: experimental evidence for the physical mechanism of the formation of a jam. *New Journal of Physics*, 10, pp. 1–7.

Taylor D. & Davis W.J. (1999) Review of basic research in bicycle traffic science, traffic operations and facility design. *Transportation Research Record 1674*, pp. 102-110.

Yao, D., Zhang, Y. Li, L., Su, Y., Cheng, S. & Xu, W. (2009). Behavior modeling and simulation for conflicts in vehicles-bicycles mixed flow. *IEEE Intell. Transp. Syst. Mag*., vol. 1, no. 2, pp. 25–30.

Zhang, J., Klingsch, W., Schadschneider, A. & Seyfried, A. (2011). Transitions in pedestrian fundamental diagrams of straight corridors and T-junctions. *Journal of Statistical Mechanics: Theory and Experiment*, vol.P06004.